REPORT DOCUMENTATION PAGE

Form Approved OMB NO. 0704-0188

1. REPORT DATE (DD-MM-YYYY)	2. REPORT TYPE	3. DATES COVERED (From - To)
12-10-2012	Final Report	1-Feb-2009 - 31-Jan-2011

4. TITLE AND SUBTITLE

Performance Improvements in Flexible Photovoltaic Technologies for Military Technology

5a. CONTRACT NUMBER

5b. GRANT NUMBER

W911NF-09-C-0037

5c. PROGRAM ELEMENT NUMBER

622705

6. AUTHORS

Steve Braymen, Frank Jeffrey, Dan Stieler, Kelly Junge, Jason Hauschildt

5d. PROJECT NUMBER

5e. TASK NUMBER

5f. WORK UNIT NUMBER

7. PERFORMING ORGANIZATION NAMES AND ADDRESSES

PowerFilm Inc.
2337 230th St.

Ames, IA 50014 -

8. PERFORMING ORGANIZATION REPORT NUMBER

9. SPONSORING/MONITORING AGENCY NAME(S) AND ADDRESS(ES)

U.S. Army Research Office
P.O. Box 12211
Research Triangle Park, NC 27709-2211

10. SPONSOR/MONITOR'S ACRONYM(S)

ARO

11. SPONSOR/MONITOR'S REPORT NUMBER(S)

55350-CH.1

12. DISTRIBUTION AVAILIBILITY STATEMENT

Approved for Public Release; Distribution Unlimited

13. SUPPLEMENTARY NOTES

The views, opinions and/or findings contained in this report are those of the author(s) and should not contrued as an official Department of the Army position, policy or decision, unless so designated by other documentation.

14. ABSTRACT

Thin film amorphous silicon photovoltaic, PV, modules can provide an efficient, light weight and conformal renewable energy source to supplement/replace existing electrical generators. The fuel delivery for these generators, particularly to forward operating bases, can be quite costly and can put men and equipment at risk of attack. Additionally, portable solar can be advantageous for civilian emergency response teams involved with natural disaster recovery actions where resources have become scarce.

15. SUBJECT TERMS

improvement flexible solar power photovoltaic

16. SECURITY CLASSIFICATION OF:			17. LIMITATION OF ABSTRACT	15. NUMBER OF PAGES	19a. NAME OF RESPONSIBLE PERSON
a. REPORT	b. ABSTRACT	c. THIS PAGE			Steve Braymen
UU	UU	UU	UU		19b. TELEPHONE NUMBER: 515-292-7606

Report Title

Performance Improvements in Flexible Photovoltaic Technologies for Military Technology

ABSTRACT

Thin film amorphous silicon photovoltaic, PV, modules can provide an efficient, light weight and conformal renewable energy source to supplement/replace existing electrical generators. The fuel delivery for these generators, particularly to forward operating bases, can be quite costly and can put men and equipment at risk of attack. Additionally, portable solar can be advantageous for civilian emergency response teams involved with natural disaster recovery actions where resources have become scarce.

Research and development opportunities to improve performance of the amorphous silicon solar material include improvements to the recombination/tunnel junction, the P+ layer deposition, and to the light collection efficiencies. The tandem PV device relies on the junction between the interface between the bottom and top layers of the tandem PV material to pass electrical current. Because of this being a reverse biased diode, a tunnel junction is created to allow for current to pass through. This junction has a voltage loss associated with it which can be improved upon thereby increase the over all device performance. The rate at which PV material can be processed through the silicon machine is limited by the rate at which a suitable P+ layer can be deposited. Improved deposition rate of this P+ layer will allow for the improved production of PV at a reduced cost. Improved light collection efficiencies would increase the power output of the PV device thereby reducing size, weight and complexity of installed power.

Enter List of papers submitted or published that acknowledge ARO support from the start of the project to the date of this printing. List the papers, including journal references, in the following categories:

(a) Papers published in peer-reviewed journals (N/A for none)

Received Paper

TOTAL:

Number of Papers published in peer-reviewed journals:

(b) Papers published in non-peer-reviewed journals (N/A for none)

Received Paper

TOTAL:

Number of Papers published in non peer-reviewed journals:

(c) Presentations

Number of Presentations: 0.00

Non Peer-Reviewed Conference Proceeding publications (other than abstracts):

Received Paper

TOTAL:

Number of Non Peer-Reviewed Conference Proceeding publications (other than abstracts):

Peer-Reviewed Conference Proceeding publications (other than abstracts):

Received Paper

TOTAL:

Number of Peer-Reviewed Conference Proceeding publications (other than abstracts):

(d) Manuscripts

Received Paper

TOTAL:

Number of Manuscripts:

Books

Received Paper

TOTAL:

Patents Submitted

Patents Awarded

Awards

Graduate Students

NAME	PERCENT_SUPPORTED

FTE Equivalent:
Total Number:

Names of Post Doctorates

NAME	PERCENT_SUPPORTED

FTE Equivalent:
Total Number:

Names of Faculty Supported

NAME	PERCENT_SUPPORTED

FTE Equivalent:
Total Number:

Names of Under Graduate students supported

NAME	PERCENT SUPPORTED

FTE Equivalent:

Total Number:

Student Metrics

This section only applies to graduating undergraduates supported by this agreement in this reporting period

The number of undergraduates funded by this agreement who graduated during this period:	0.00
The number of undergraduates funded by this agreement who graduated during this period with a degree in science, mathematics, engineering, or technology fields:.....	0.00
The number of undergraduates funded by your agreement who graduated during this period and will continue to pursue a graduate or Ph.D. degree in science, mathematics, engineering, or technology fields:.....	0.00
Number of graduating undergraduates who achieved a 3.5 GPA to 4.0 (4.0 max scale):	0.00
Number of graduating undergraduates funded by a DoD funded Center of Excellence grant for Education, Research and Engineering:	0.00
The number of undergraduates funded by your agreement who graduated during this period and intend to work for the Department of Defense	0.00
The number of undergraduates funded by your agreement who graduated during this period and will receive scholarships or fellowships for further studies in science, mathematics, engineering or technology fields:	0.00

Names of Personnel receiving masters degrees

NAME

Total Number:

Names of personnel receiving PHDs

NAME

Total Number:

Names of other research staff

NAME	PERCENT SUPPORTED

FTE Equivalent:

Total Number:

Sub Contractors (DD882)

Inventions (DD882)

Scientific Progress

Technology Transfer

PowerFilm® Corporation
Ames, IA

Performance Improvements in Flexible Photovoltaic Technologies for Military Technology

Final Report

AMSRD-ARL-RO-SI Proposal No. 55350-CH

Agreement No. W911NF-09-C-0037

For period January 08, 2009 through January 31, 2011

Submitted by
Steven Braymen
PowerFilm Solar, Inc.
2337 230th St.
Ames, IA 50014

Table of Contents

back metal surface. Purchase and/or modify equipment and procure required materials and supplies, including sputtering targets and reactive gases. This will be an on going process through out the project as the importance of individual or unexpected variables are identified.

3.2 Develop operating parameters using suitable candidates found in 3.1. Characterize the suitability of design and materials for PV material. Build initial tests devices and characterize their performance.

3.3 Incorporate the best solutions into a PV module and run comparative testing against standard modules.

Task 4: I-Layer/ P: I Interface Improvement

4.1 Establish deposition characteristics of the I layer for each electrode in the new, multiple electrode system considering deposition rate and rate at which the deposition moves to the more ordered "proto-crystalline" and micro-crystalline structures. This will be evaluated particularly relative to power and hydrogen dilution.

4.2 Determine effects of differential gas flows through the different electrodes and effective mixing of gases in the system for the gas concentrations an silane depletion appropriate for intrinsic a-silicon deposition. This will be used to identify whether a physical barrier is needed between electrodes to achieve differentials in silane partial pressures between areas.

4.3 Develop parameters that moves the film structure to the more ordered "proto-crystalline" and micro-crystalline and establish how deposition parameters may be used to control that transition.

4.4 Apply parameters developed in 4.3 to the final electrode in the multiple electrodes, I layer deposition zone to create a proto-crystalline layer at the top interface of the I-layer. Develop optimum rate parameters to optimize voltage in full devices. Identify parameter limits needed to protect against overshooting to a microcrystalline structure that would cause voltage to drop dramatically.

Task 5. Module fabrication using improvements

5.1 Produce and test a PV module with the best solution identified and developed for the top conductive oxide.

5.2 Produce and test a PV module with the best solution identified and developed for the P+ layer.

5.3 Produce and test a PV module with the best solution identified and developed for the red response.

5.4 Produce and test a PV module with the best solution identified and developed for the improved I-P+ interface.

5.5 Compile all of the inter-compatible improvements into a single module.

Task 6 Fabrication of tent deliverable

6.1 Fabricate and a 2KW PowerShade using the PV modules produced in 5.5.

Figures and Tables

Statement of Problem

Relevance to Army

Thin film amorphous silicon photovoltaic, PV, modules can provide an efficient, light weight and conformal renewable energy source to supplement/replace existing electrical generators. The fuel delivery for these generators, particularly to forward operating bases, can be quite costly and can put men and equipment at risk of attack. Additionally, portable solar can be advantageous for civilian emergency response teams involved with natural disaster recovery actions where resources have become scarce.

Research and development opportunities to improve performance of the amorphous silicon solar material include improvements to the recombination/tunnel junction, the P+ layer deposition, and to the light collection efficiencies. The tandem PV device relies on the junction between the interface between the bottom and top layers of the tandem PV material to pass electrical current. Because of this being a reverse biased diode, a tunnel junction is created to allow for current to pass through. This junction has a voltage loss associated with it which can be improved upon thereby increase the over all device performance. The rate at which PV material can be processed through the silicon machine is limited by the rate at which a suitable P+ layer can be deposited. Improved deposition rate of this P+ layer will allow for the improved production of PV at a reduced cost. Improved light collection efficiencies would increase the power output of the PV device thereby reducing size, weight and complexity of installed power.

Approach

- The tunnel junction can be modified by adding a material that forms a recombination layer between the top and bottom layer of the tandem PV device. This will produce an ohmic contact there-by overcoming a built-in voltage bias loss at this junction.

- A new antenna configuration will be utilized to deposit microcrystalline structured P+ material at an enhanced rate. This configuration will allow for the nucleation of the preferred crystal structure, which is the slow step, and then deposit the bulk of the layer at an enhanced rate. Additionally, the I, or intrinsic, layer material deposition parameters will be modified to provide for a micro-crystalline template to further enhance the P+ properties.

- Both the top conductor and the back metal interface will be modified to maximize the amount of light entering the PV material and reflected. Optical transparency and anti-reflective properties can be altered to maximize light absorption. At the back metal interface, maximum reflection and light scattering can be optimized.

Summary of most important results

Modification to the top conducting oxide, TCO, layer produced material that qualified Power Film's photovoltaic, PV, material as a durable 20+ year lifespan module this material, passing the1000h hour 85C/85%RH damp heat test as detailed in the IEC61646 regulations.

Modification to the back metal substrate texture improved the current by as much as 9% over standard material. Although this improvement was found to be cost prohibitive.

Improvements in the P+ layer deposition rate have significantly improved production rate of the PV material through the silicon deposition process by 60%. The silicon deposition process is rate limiting in a series of processes required to manufacture PV modules. This reduction in process time results in savings primarily in electricity use of up to 50 % per foot of PV produced, and in labor for this process. Future capital expenditure for plant capacity expansion is also expected to be reduced.

Identified optimum conditions and thickness for the I1 layer.

Improved tunnel/recombination junction has resulted in a voltage of nominally 1.6 to 1.7 volts per cell in the tandem material.

Material was manufactured into a 2KW Power Shade.

Task 1: Top Conductive Oxide Improvement

Purpose of this task is to reduce the front surface reflection and minimize absorption in the top conducting oxide (TCO). ITO can be sputter deposited leaving an antireflective thin film of suitable conductivity to be useful for photovoltaic, PV, devices. The sputter process is a relatively slow process limiting through put in our roll to roll process. Multiple targets can be utilized to increase this through put at the cost of additional engineering and capital equipment. Alternatively, a superimposed RF-DC sputtering technique may be employable to boost the deposition and through put rates.

1.1 Design, acquire and set up RF/pulsed DC power mixing system for sputter deposition to run on existing experimental chamber. Test and develop operating procedure.

An Advanced Energy's Pinnacle Plus DC power supply, a Dressler's Pinnacle Plus RF power generator and an Advanced Energy's low pass filter mixing system were acquired.

These instruments were installed and tested, allowing testing of RF, DC, pulsed DC, and RF superimposed on DC in a sputter operation. Figure 1.1.1 shows a block diagram of the deposition system and arrangement of the supplies and filter.

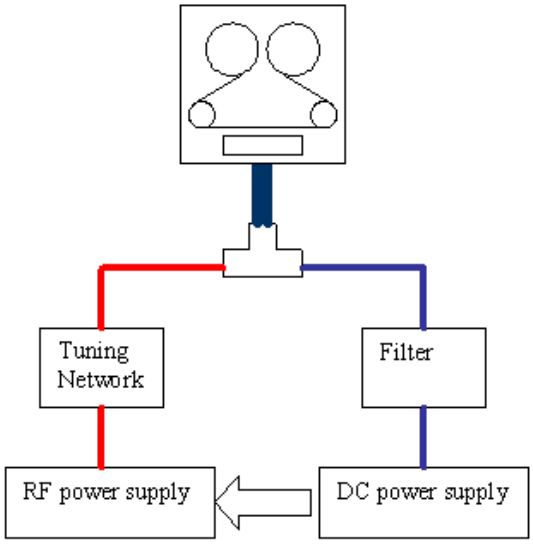

Figure 1.1.1 Sputter deposition chamber with RF-DC supplies configuration.

The RF tuning network prevents the DC power supply from damaging the RF power supply. Conversely, the filter prevents damage to the DC power supply from the RF. Arc suppression is accomplished through the DC power supply controlling the RF supply's output. Arc suppression prevents damage to the power supply circuit and the sputter source target. Figure 1.1.2 diagrams the schematic of the setup.

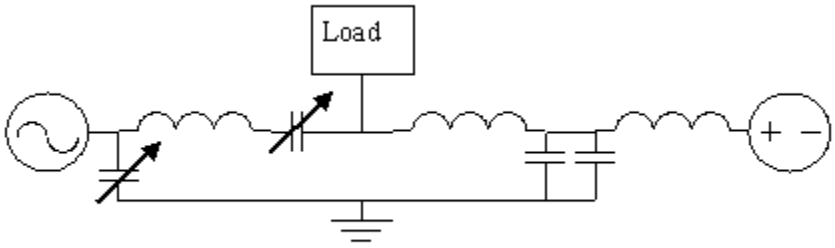

Figure 1.1.2 Schematic of the RF-DC sputtering apparatus.

Testing parameters investigated for this system were substrate temperature, post process annealing, frequency of pulsed DC power, chamber pressure, and distance from the target, and RF superimposed on to DC.

The substrate was heated during the deposition process using a block heater in contact with the back of the web. It was determined that heating the web during the deposition of the ITO had no affect on device performance.

A post annealing cycle, 5 minutes at 145C, improved the device performance and dramatically decreases the sheet resistance of the ITO layer when deposited using DC and Pulsed DC power. RF biased DC sputtering did not show an improvement when annealed. This was determined to be a side effect of the RF biased DC sputtering causing a large temperature rise of the substrate, effectively annealing the film in-situ.

The DC sputtering technique, the pulse rate frequency did not show any measurable influence on device.

The spacing of the sputtering target source material to the web was investigated. The sheet resistivity was found to increase with spacing, figure 1.1.3. The web temperature was found to decrease with spacing.

Pressure had little effect on the deposited material properties using the DC process above 3.0 mTorr. Unfortunately it was not possible to measure the effects of pressure with the RF biased DC sputtering. This technique resulted in the web heating to the point of failure and the out-gassing product of the web and ink. This out-gassing caused unstable pressure readings and interfered with the process.

Figures 1.1.3 through 1.1.6 are a series experiment which gives PV module output power as a function of the distance of web to the target for given pressures. It has been found that pressures of about 4.0 mTorr and with a 4 inches web to target separation, at higher DC powers give the better results. The presented data is at constant film thickness of about 220nm.

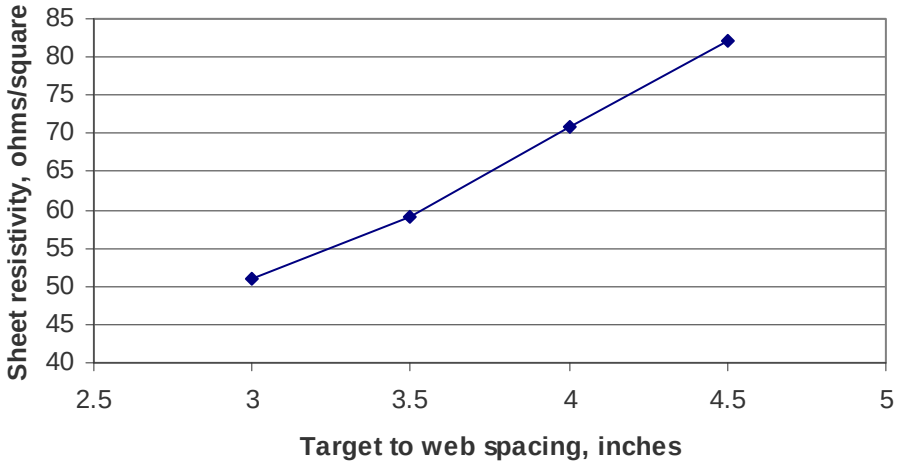

Figure 1.1.3 Sheet resistivty of the deposited ITO film as a function of target to web spacing. RF biased DC sputtering.

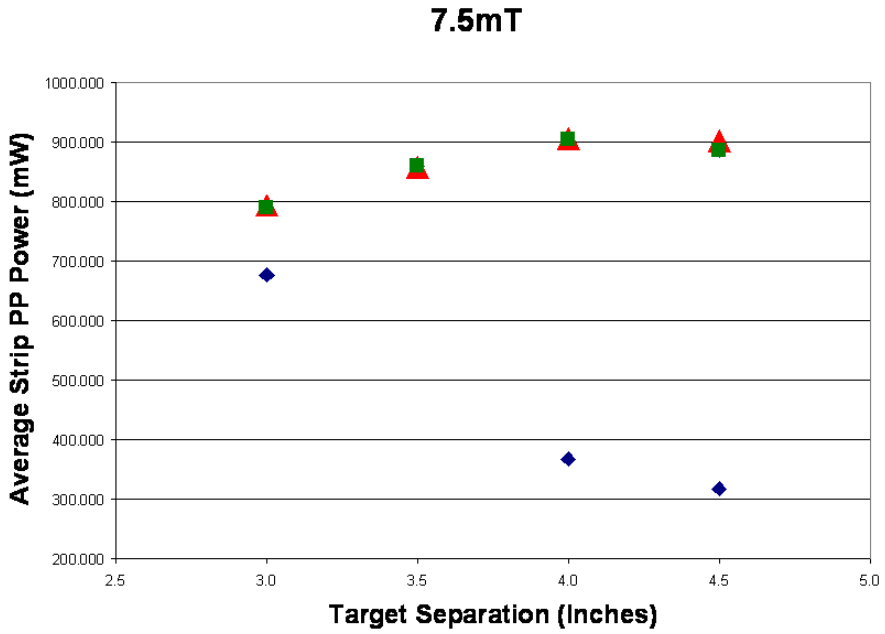

Figure 1.1.4 Average Power Point for PV modules at various target spacing and pulsed DC frequencies at a pressure of 7.5 mTorr.

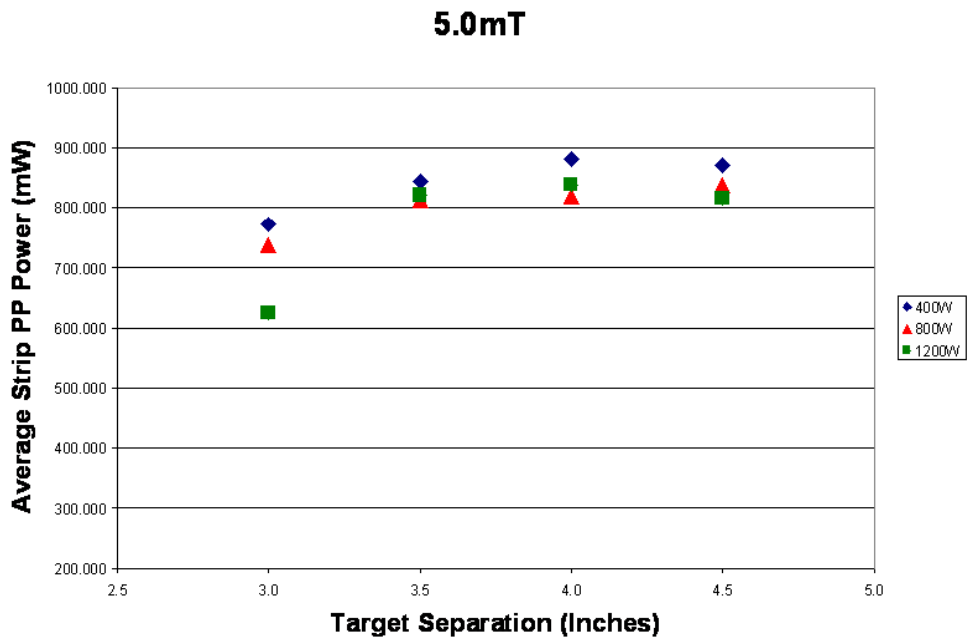

Figure 1.1.5 Average Power Point for PV modules at various target spacing and pulsed DC frequencies at a pressure of 5.0 mTorr.

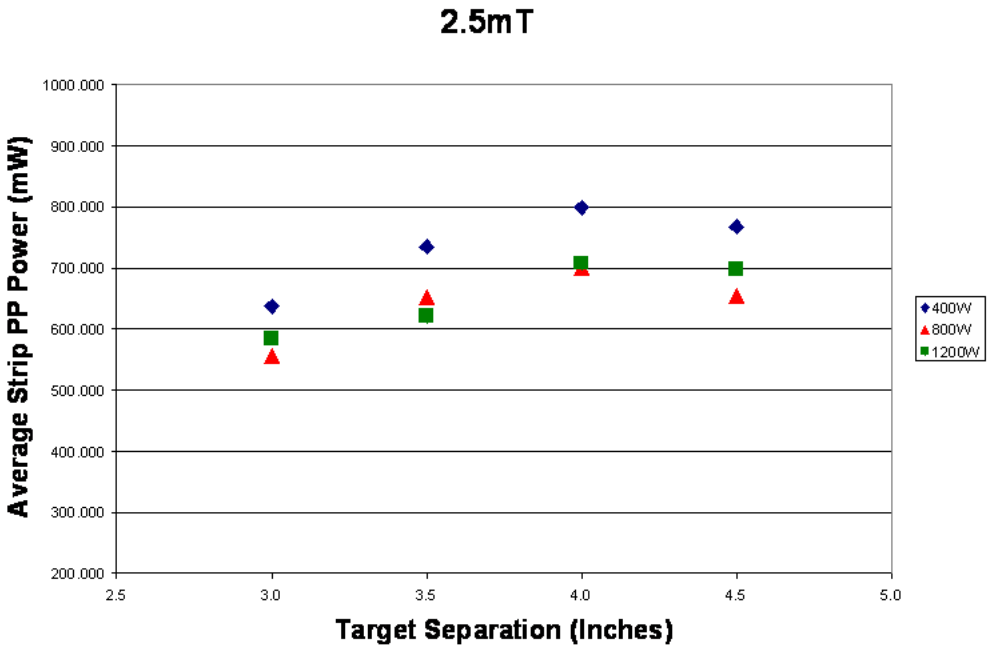

Figure 1.1.6 Average Power Point, PP, for PV modules at various target spacing and pulsed DC frequencies at a pressure of 2.5 mTorr.

RF biased pulsed DC was found to cause unstable plasma and electrical arcing issues with in the deposition system. It was found that at higher RF powers this process was more stable and arcing was be suppressed. Unfortunately this also leads to the web

substrate being subjected to conditions which caused extreme temperatures, resulting in the web and insulator inks to char and decompose. These problems dominated device performance. It was not possible to overcome this heating problems with RF superimposed on the pulsed DC.

The ITO use as a sputtering source material is plagued by problem on nodule growth on the face of the material. These nodules interfere with the yield and quality of the resulting film. It is known that lower target bias voltages reduce this nodule growth. Additionally, lower bias voltages can produce films with lower resitivities. It was found that a RF biasing can reduce the voltage on the target with a minimum around 500 watts RF, figure 1.1.7. This will be useful information when a solution to the web over heating is found.

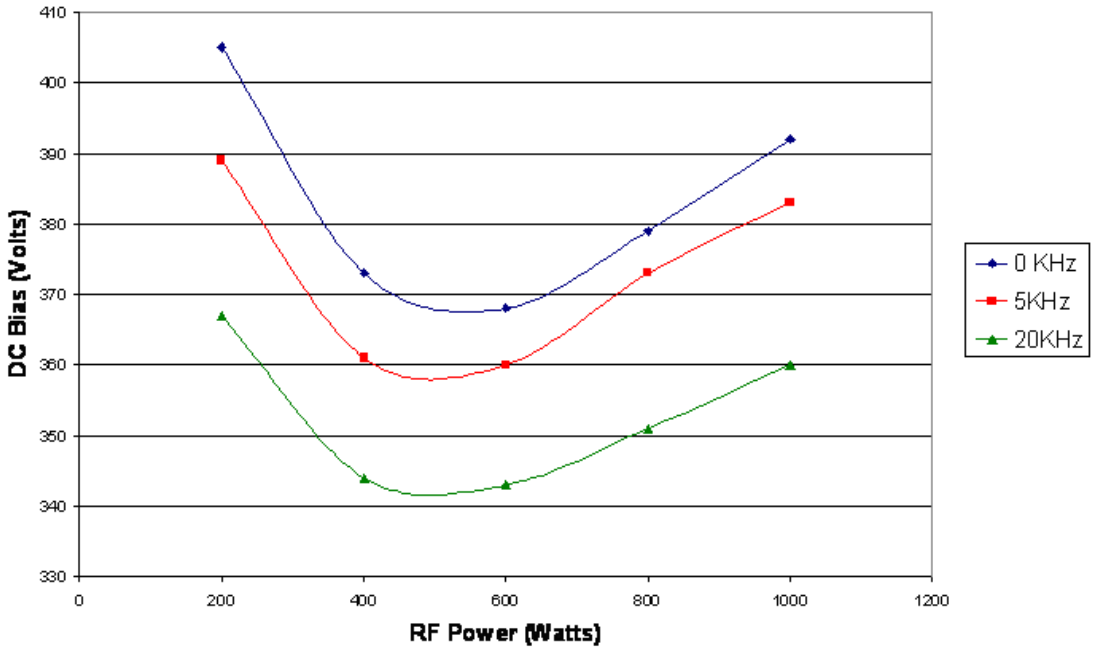

Figure 1.1.7 DC Bias voltage at various RF powers and Pulsed DC frequencies showing the minimum at a power ratio of 1.2 DC:RF. 5 mTorr pressure and 3.0 inch separation.

Additionally, the RF system was generally unstable with large reflected powers common. It is believed that as total power increases, the system would increasingly more stable and have a lower bias voltage. An attempt was made to verify this, however, by setting the RF supply at its maximum of 1000 watts and operating the DC supply at 2000 watts and 3000 watts. This resulted in a catastrophically failure of the target material figure 1.1.8 and charring of the web material, figure 1.1.9. Pressure climbed out of control, probably due to gases being given off by the charring of the materials.

It was found that in all cases tested, the RF/pulsed DC sputtering technique resulted in significant damage to the PV substrate and sputtering target and is no longer considered a viable process.

Future processing remained with using DC and pulsed DC sputtering as the method of choice.

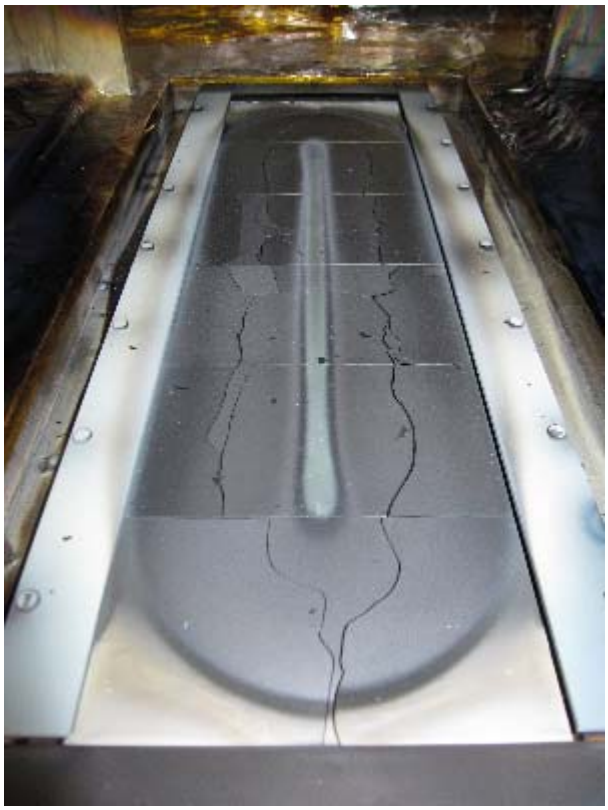

Figure 1.1.8 Picture showing damage to the ITO target.

Figure 1.1.9 Picture showing damage to the web and ink lines.

1.2 Characterize deposition of indium tin oxide, ITO, and zinc oxide, ZnO, using the above system. Variables include power, pressure, O2 flow, and RF/DC mix. Deposition and material parameters include Optical characteristics, conductivity, deposition rate and built in stress.

DC and pulsed DC sputtering has been selected as the deposition method of choice.

Film resistivity is required to be below 90 ohms per square. The ZnO was found to produce films above this maximum requirement and ZnO experiences environmental degradation problems. ITO exceeds the resistivity requirement and is environmentally stable and was therefore selected as the material to pursue.

Development of the ITO deposition process determined the power, pressure, and target to web distance as a function of module performance. The operational parameters of 1200 W, 7.5 mTorr, and 4.0" target separation were selected, figure 1.2.1.

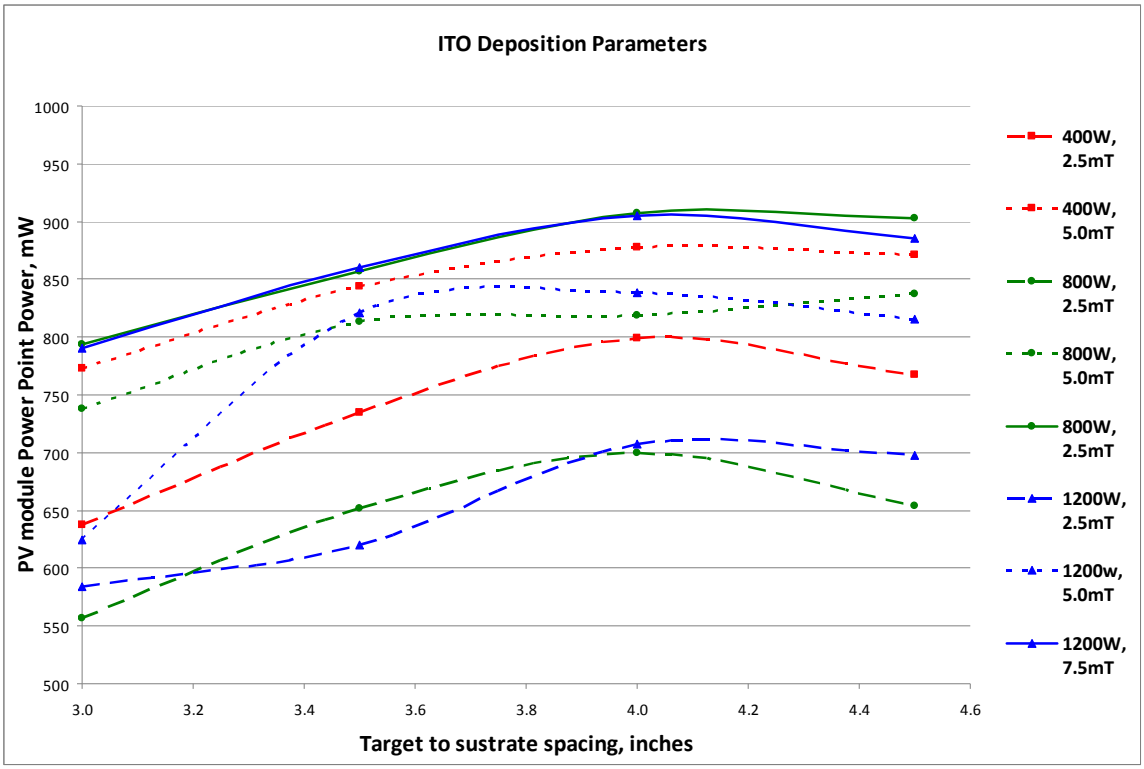

Figure 1.2.1. Results of the ITO development tests.

1.3 Apply the best candidate material from above to our PV devices. Analyze impact of variations of running conditions on device performance to optimize behavior.

Photovoltaic, PV, modules using indium tin oxide, ITO, as the primary top conductive oxide, TCO, were manufactured. To qualify as a durable 20+ year lifespan module this

material needs to pass the1000h hour 85C/85%RH damp heat test as detailed in the IEC61646 regulations.

Sections standard material runs were tested through the damp heat test. Test sections had a variety of TCO conditions, each with approximately 1/4 wavelength of total thickness. The quarter wave length acts as an anti-reflecting layer enhancing light absorption. The ITO was deposited @ 1200W with a pressure of 2.5 mTorr and a distance to target of 3" These samples showed no discernable degradation following the 1000h damp heat exposure. The best performing conditions had a 4" to target ITO spacing. Ultimately, the sputtering conditions adopted for our production line were 1200 watts DC pulsed at 85 kHz and a 5usec pulse width for the ITO using 1% oxygen in an 8 mTorr Argon atmosphere.

Task 2: P+ Layer Improvement

The purpose of this task is to improve the P-doped silicon layer to reduce absorption losses in the blue part of the light spectrum.

2.1 Establish deposition characteristics of P+ layer for each electrode in the new, multiple electrode system.

The configuration of the multi-antenna system has two antennas within the same deposition zone. Each antenna has its own RF power source as well as independent gas supplies. To produce P+ silicon requires silane, SiH4, and diborane, B2H6, reactant gases. RF power is applied and the appropriate thickness of P+ layer is deposited.

The multi-antenna system was operated to confirm uniformity with the deposition with equal thickness films deposited from each antenna building the total required film thickness.

The target thickness of this layer was 35nm. Initially, the RF powers to each antenna were held constant at 1000 watts RF using a 75% duty cycle. Devices obtained with these conditions show a large barrier which dropped the voltage and diminished the fill factor to below acceptable levels.

This material, as under performing as it was, established a base line performance.

2.2 Determine effects of differential gas flows through the different electrodes and effective mixing of gases in the system for condition appropriate for microcrystalline silicon deposition. This will be used to identify whether a physical barrier is needed between electrodes to achieve differentials in silane partial pressures between areas.

The RF power levels to each antenna were optimized. It was found that as the power increases, so does the PV performance, however, the system is limited by the maximum output available from the current RF power supplies. There appears to be little advantage

to having different powers applied to the separate antennas. More power is always better up to the 1100 watt limit of our power supplies.

A study was conducted to determine the optimum gas flow to each antenna with in the P+ zones. The hydrogen flow was set to obtain and control the process pressure with the dilution ratio appropriate for depositing micro-crystalline silicon. The silane gas flow was split between each of the two antennas with in the zone. To produce a P+ layer of 35nm in thickness for a web speed of 3 inches per minute, 13 sccm of silane total between the two antennas is required. Test were done with the silane gas split between the two antennas with a ratio that varied from 13:0 to 0:13. The ratio 13:0 represents all of the silane going to the "A" antenna and no silane going to the "B" antenna.

This study showed that the better performing PV material is produced when only hydrogen flows through the "A" antenna and a hydrogen-silane blend flow through the "B" antenna, figure 2.2.1, 2.2.2.

Additionally, it was determined that no physical barrier was necessary.

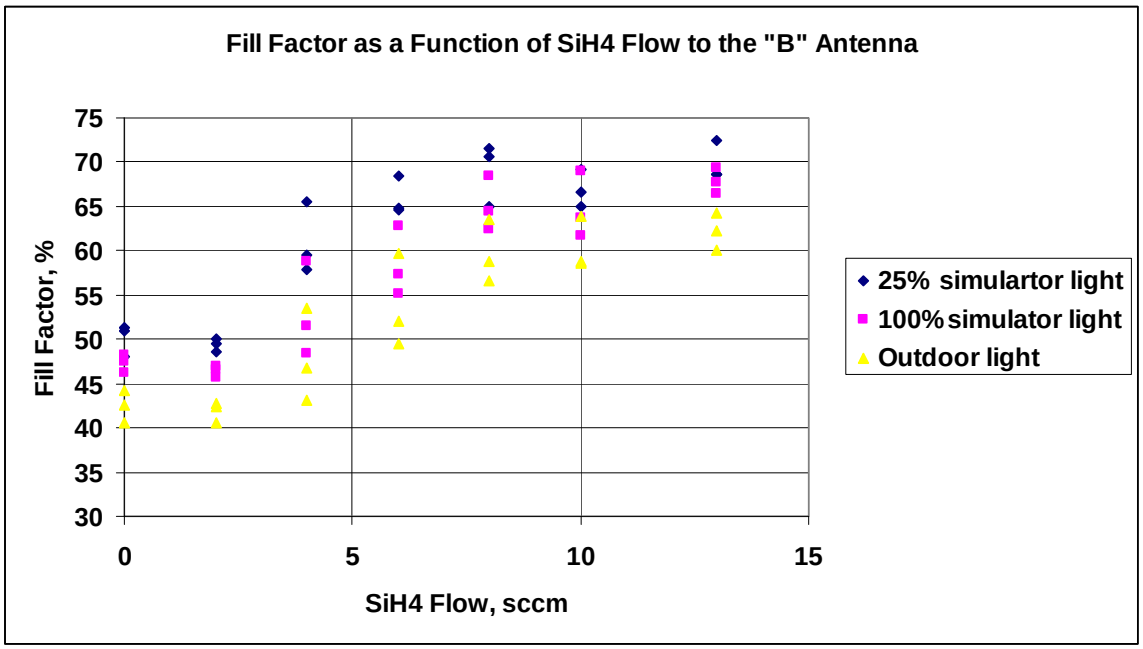

Figure 2.2.1. Fill factor of full modules as a function of silane flow to the "B" antenna with the total combined silane at 13 sccm.

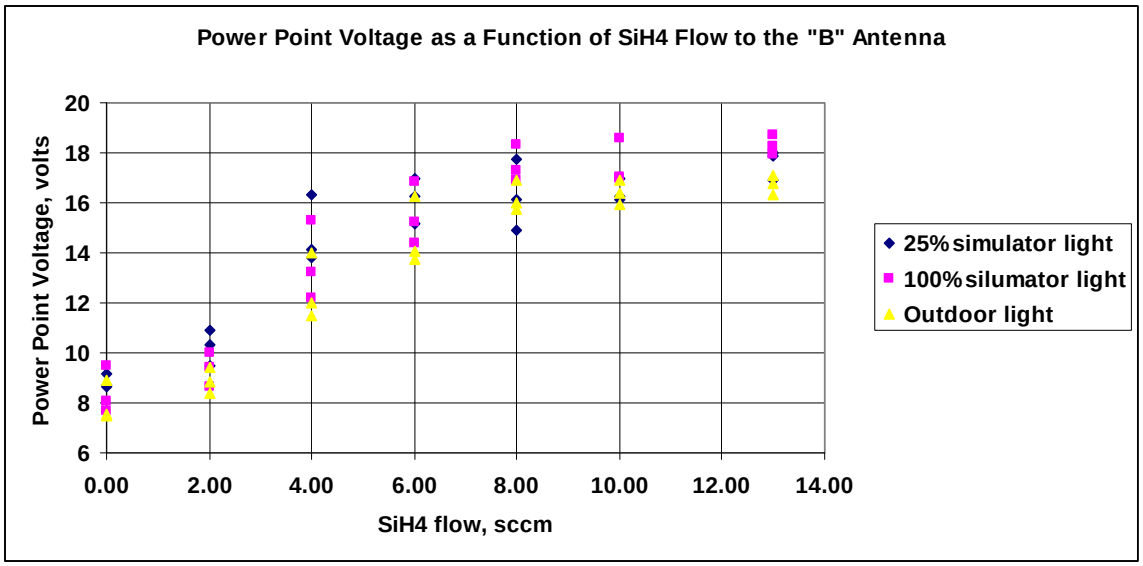

Figure 2.2.2. Power Point Voltage of full modules as a function of silane flow to the "B" antenna with the total combined silane at 13 sccm.

A procedure to test individual layers by measuring light/dark conductivities and activation energies of carriers was developed and implemented. This technique allowed for fast return on test results for the boron doped P+ layer thin films with out the need to produce full PV devices. This technique was also successfully applied to the N+ and I-layer thin films.

For doped films a light/dark conductivity ratio should be close to unity and the activation energy as low as possible. With this techniques it was confirmed that it the best deposition condition is for the P+ material is when the silane flowed only to the B antenna, figure 2.2.3.

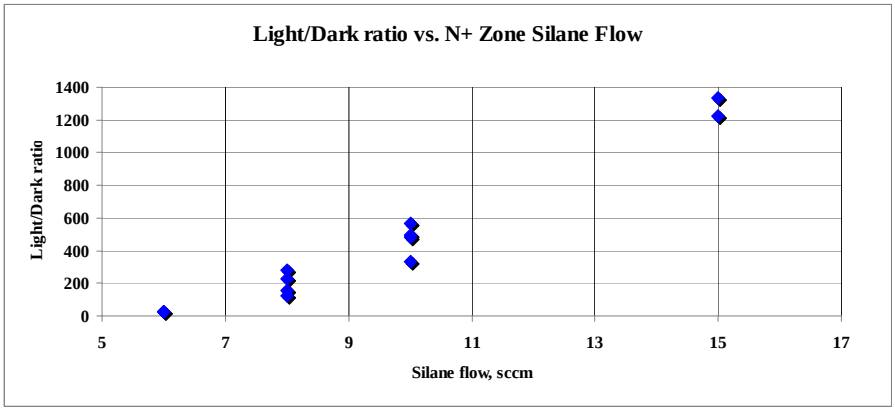

Figure 2.2.3. A plot of light/dark conductivity ratio versus Silane flow for N+ material demonstrating the effectiveness of this measuring technique.

2.3 Develop parameters to enhance the transition from amorphous to microcrystalline deposition and establish how deposition parameters may be used to control that transition.

In addition to a hydrogen gas flow, it has been determined that the RF is required at the A antenna even though there was no deposition. When the RF power is applied to the hydrogen at the A antenna, etching of the I-layer prepares the surface so that the P+ layer to grow as micro-crystalline. With this method, the Voc of the PV has increased to greater then 1.8 volts per cell giving a 12-cell module, a gain of nearly 2 volts over all. Because the system is normally operated near the upper limits of the power supplies, the range of testing was limited. It can be seen that the fill factor improves as the power in the P+ zones is increased, figure 2.3.1. This test was limited to 1200 watts by the maximum output of the available RF power supplies.

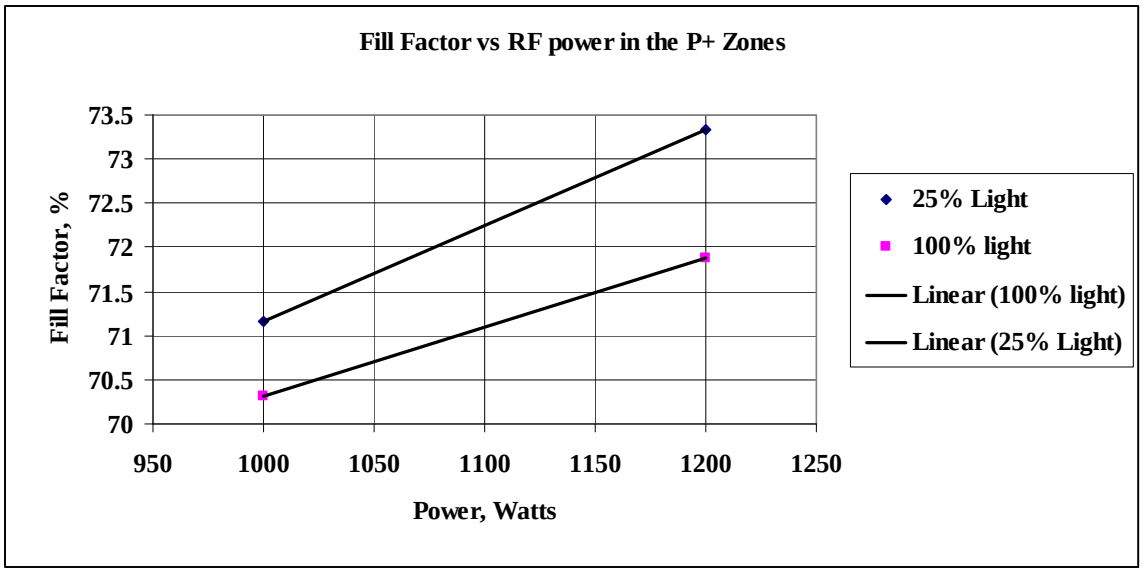

Figure 2.3.1. Fill Factor versus RF power applied to the P+ antennas.

In single antenna machines, such as the 13" wide machines, the conditions of deposition of the intrinsic layer affect the voltage of the PV device. This is due to the growth of the I-layer with structure approaching microcrystalline, u-xtal, being preferred. This structure can be controlled using flow, power, and pressure. It was found that the Voc of the PV material is not affected by the deposition I-layer conditions in the MW machine when the P+ box is run as described above. It is believed that the hydrogen etching, conditions the I-P interface sufficiently to maximize the voltage output and allowing for a broader range of deposition conditions. The goal for the I-box conditions became that of cross web uniformity.

The output of the power supplies can be controlled, not just with the power output, by pulsing the out put at a user selectable frequency with a user selectable duty cycle, or percent on time. For high power usage, it is best to pulse the output. This allows the charge build up on the web to dissipate with out arcing and causing damage to the web

material. This pulse rate was set to 1000Hz. In addition, the duty cycle, or on time of each pulse, is user addressable and was set to 75%.

Because it was determined that the best PV resulted from the RF power levels at a maximum, the duty cycle was changed to maximize the total power delivered, i.e. highest possible on-time, with out damage causing discharges. The higher total power would also tend to improve deposition rate and the microcrystalline structure of the film. Tests were run at 75%, 85%, 95%, and 100% (unpulsed) on-time. First it was confirmed that the pulsed duty cycle is necessary for our process not to damage the web material. Additionally it was found that the material properties did not change significantly at any pulse rate, figure 2.3.2. However the deposition rate of the silicon film, did increase as the duty cycle was increased, allowing for faster web speeds for production.

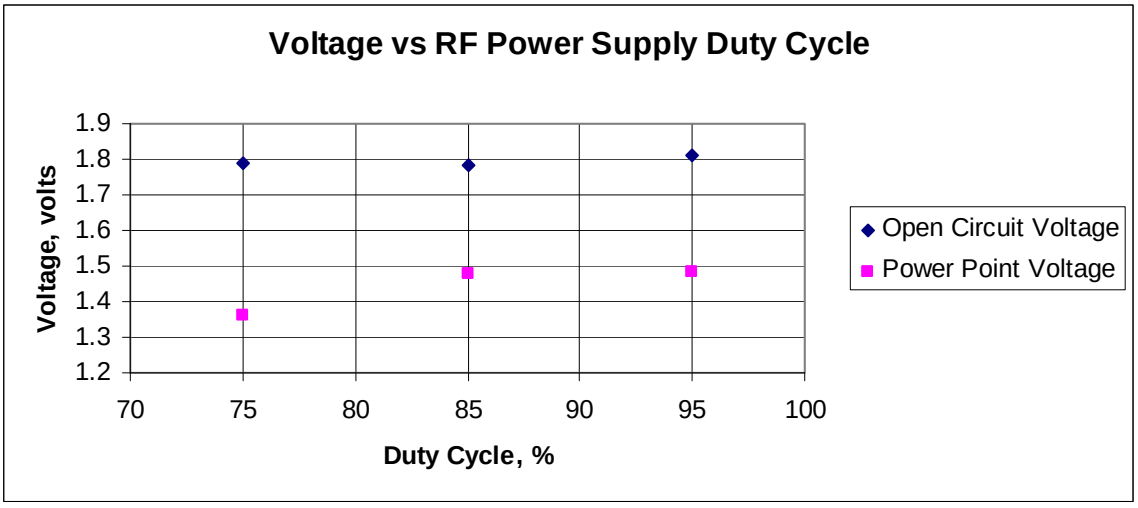

Figure 2.3.2. Device voltage per cell versus the RF power supply duty cycle.

2.4 Apply parameters developed in 2.3 to initial electrode in multiple electrode system to create microcrystalline "template" for faster deposition of microcrystalline material in by the second electrode. Develop optimum rate parameters to minimize optical loss in the combined layer and maximum effective deposition rate.

PV modules have been produced at 4"/min with performance that exceed the standard for the products being manufactured. This is an increase in production of 33%. Small samples of device material have been produced up to 5"/min with good results. Because of the limitations of the maximum output of the RF power supplies and the current size of the gas flow controllers, this is believed to be the practical operational limit for this machine.

Pushing this system to a maximum through out rate found that at 5"/min, the PV material exhibited an electrical barrier that reduced the current at the power point to below acceptable levels. This loss was attributed to a loss of the micro-crystallinity of the P+

layer. This causes both an interface issue with the top conducting oxide and absorption of the blue light preventing it from contributing to the current generation.

Micro-crystallinity of the P+ relies on the dilution of the silane by the hydrogen during deposition and the RF power to provide a back etch. As the web rate is increased, the required silane flow is also increased, decreasing the hydrogen:silane ration making it less likely to grow the preferred structure. It was additionally found that the diborane interferes with the micro-crystalline growth. A study was performed to identify the optimum diborane flow. Up to this point, the diborane flow was set to 2% of the silane flow. It was found that this was excessive and that at a 0.5% diborane flow produces material significantly improved performance, figure 2.4.1.

With optimizing these parameters, PV material performing above specifications can be produced at 5 inches per minute web speed. This is an improvement of over 60% from our standard process.

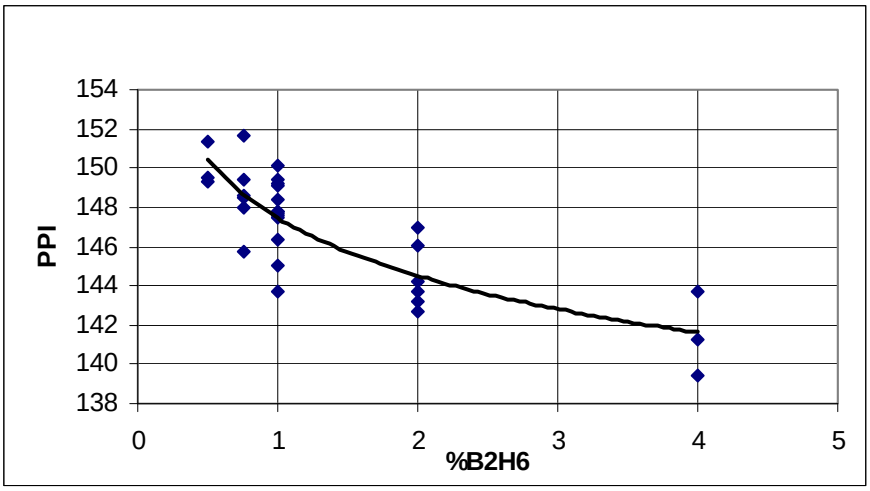

Figure 2.4.1. Power point current, PPI, as a function of diborane flow as a percent of silane flow.

It was thought possible to translate the parameters of hydrogen etching prior to P+ deposition to the standard 13 inch wide machines.

In one of our standard silicon deposition machines, the P1 box's gas flow distribution was modified to allow for hydrogen only to go to the first half of the antenna and hydrogen, silane and diborane to the second half of the antenna. Barriers were installed to segregate the flows regions. Tandem material was produced and tested for fill factor and Voc. Although results were mixed, the data shows higher Voc and similar FF for the 750W condition, as compared to standard 13 inch tandem PV. The higher RF powers did not test as well and may indicate an upper limit of PV performance when using this technique for deposition.

Condition	Voc	FF	Light Intensity	RF Power	Hydrogen Flow 1st half / 2nd half

Test	1.756	61.428	100%	750W	550/1100
Test	1.436	44.944	100%	900W	550/1100
Test	1.665	65.683	25%	750W	550/1100
Test	1.398	57.026	25%	900W	550/1100
Standard	1.651	61.858	100%	750W	1100
Standard	1.546	62.186	25%	750W	1100

Table 2.4.1, Data from a 13" machine modified to hydrogen etch the I-layer prior to P+ deposition.

Task 3: Red Response Improvement

The purpose of this task is to increase the collection of light in the red part of the spectrum.

3.1 Identify applicable technologies, geometries, and necessary characteristics of materials that will be used to enhance the reflection of the red spectrum off the back metal surface. Purchase and/or modify equipment and procure required materials and supplies, including sputtering targets and reactive gases. This will be an on going process through out the project as the importance of individual or unexpected variables are identified.

Sputter deposited chrome nitride, CrN, has been identified as an alternative for use as a back reflector layer. The absorption curve is much more favorable for this purpose, figure 3.4, see below.

Additionally, the texture created by the aluminum back conductor metal has been identified as an area of potential light collection improvement. In addition of the being the back current collector, this metal acts as a reflector of light passing through the PV stack. When textured, the reflected light can be scattered by a texture, roughness, giving the light a better chance of being absorbed on its return trip out of the PV material.

3.2 Develop operating parameters using suitable candidates found in 3.1. Characterize the suitability of design and materials for PV material. Build initial tests devices and characterize their performance.

Red Light Back Reflector

To improve the performance of the PV modules, it would be beneficial to use all available photon that is incident onto the cell. Light intensity as a function of depth (x) can be described with the following equation.

$$I = I_o e^{-\alpha x}$$

Where

$$\alpha = 4 * \pi * N * K / \lambda$$

The parameters N & K are the complex refractive index of the material in which the light is moving and λ is the wavelength of the light in question. The complex refractive index for amorphous silicon (a-Si), figure 3.2.1..

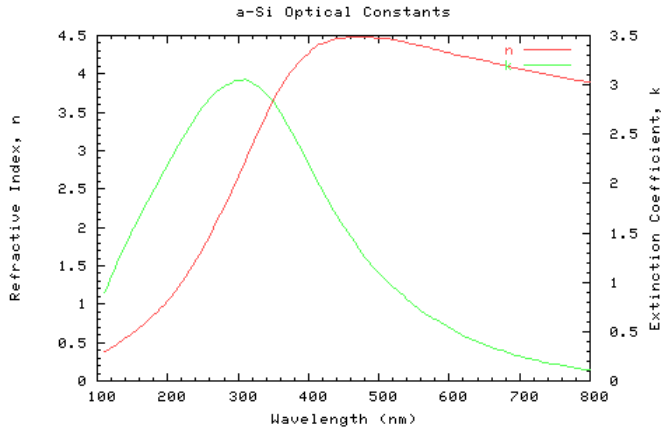

Figure 3.2.1 A penetration depth ($x=1/\alpha$) can be calculated for each wavelength where the light intensity has fallen by a factor of 1/e.

The penetration depth graph shows that the red section of the wavelength spectrum can travel much farther through a-Si than the blue, figure 3.1.2. This leaves only the red light to reflect back through the PV material, giving it a second chance to be absorbed by the active layers.

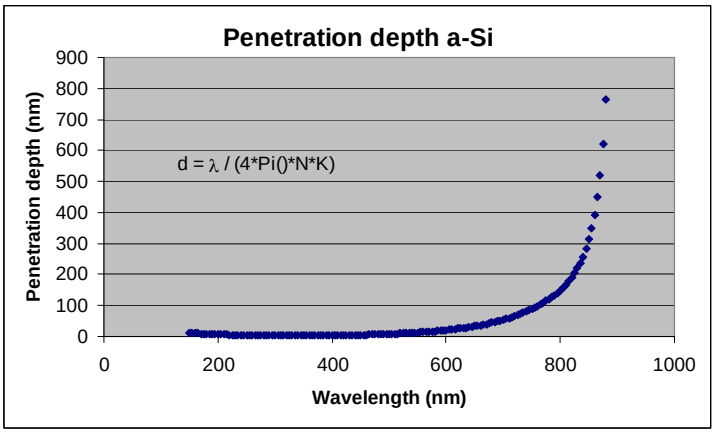

Figure 3.2.2. Penetration depth as a function of wavelength for light in silicon PV material.

As standard, a thin layer of Titanium Nitride, TiN, to cap our bottom metal stack. This layer prevents oxidation of the Aluminum, Al, acts as a barrier for Al diffusion into a-Si, and is a relatively good electrical conductor. However, TiN is a rather poor bottom

optical reflection/absorption layer, which can be seen in the refractive index profile, figure 3.2.3.

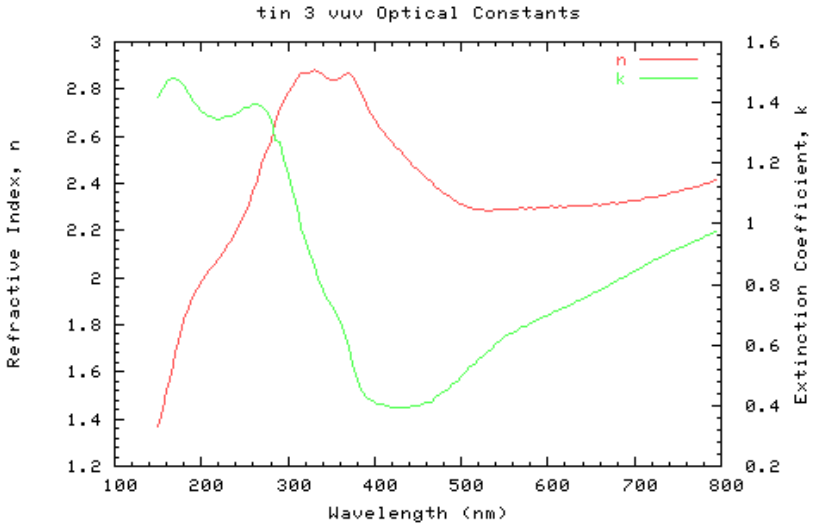

Figure 3.2.3. The extinction coefficient (k) increase with wavelength in the red end of the spectrum (600nm-800nm).

To reduce absorption the best reflective layer would have an extinction coefficient value near zero in the red region. With this chrome nitride, CrN , was identified as a potential candidate material., see figure 3.2.4.

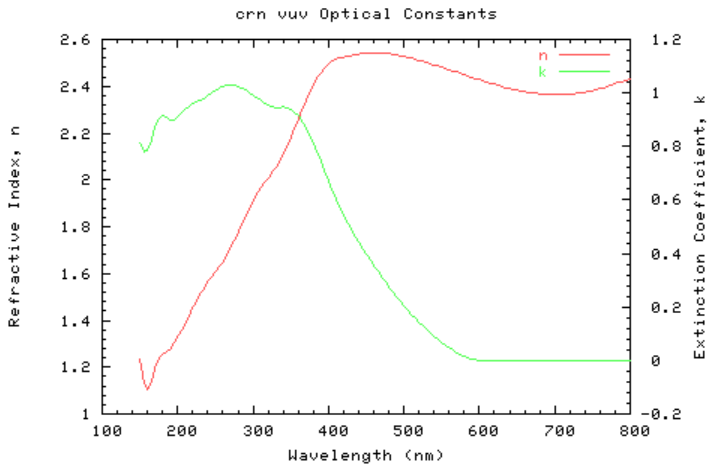

Figure 3.2.4 Optical constants of chrome nitride at various light wavelengths.

The amount of light intensity that would be returned to through the PV after reflecting off of the bottom metal stack was modeled using the absorption equations from above and the following reflection equations.

$$R = \left((n_1 - n_2) / (n_1 + n_2) \right)^2 \qquad \text{for dielectrics}$$

and

$$R = ((n_1 - n_2)^2 + k_2^2) / ((n_1 + n_2)^2 + k_2^2) \quad \text{for metals.}$$

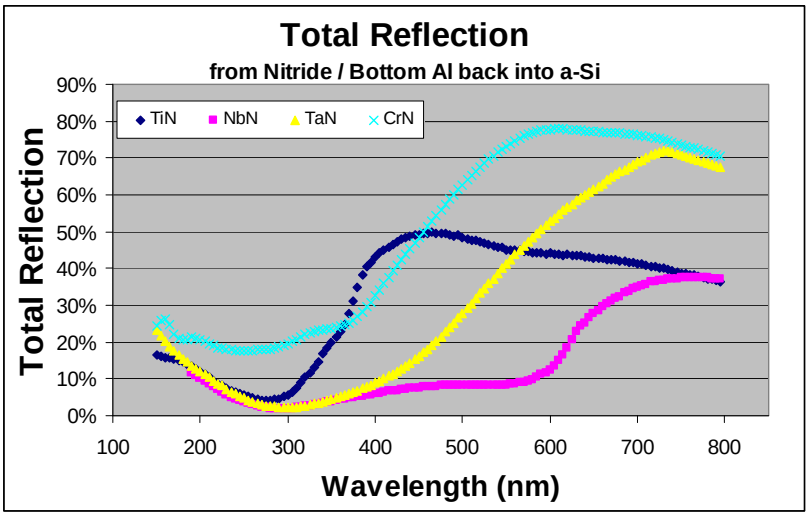

Figure 3.2.5. Comparison of optical properties of various materials of interest.

This model indicated that it is possible to nearly double the amount of red light returned through the PV by using CrN as a capping layer on the back metal.

A reactive sputtering process was developed to deposit CrN and standard PV modules were made with and with out CrN as a back reflector, on different metal substrates and aluminum purity. The pure aluminum was tested because of its higher intrinsic reflectivity. Results of this test are seen in figures 3.2.6 and 3.2.7.

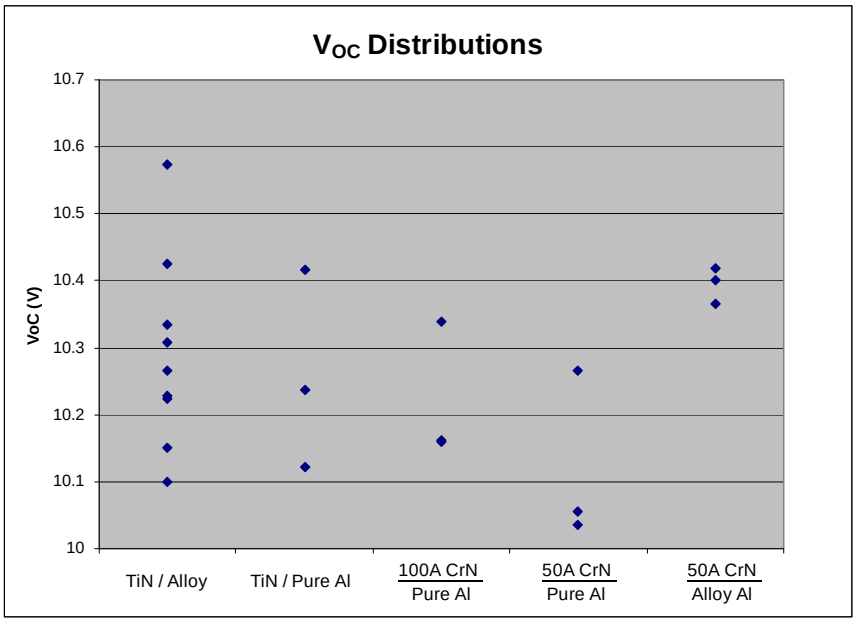

Figure 3.2.6. Open circuit voltage, Voc of the PV modules with various back reflector treatments.

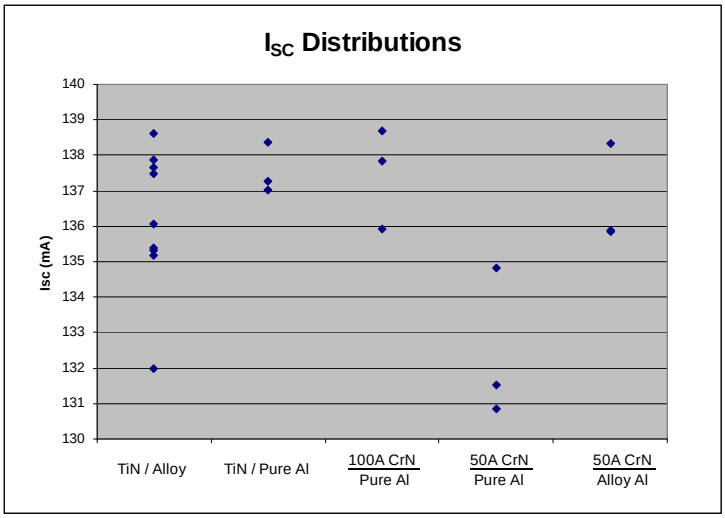

Figure 3.2.7 Short circuit current, Isc of the PV modules with various back reflector treatments.

These tests indicated no net improvement in the performance of the PV modules. A repeat of this test resulted in the same behavior. It is worth noting that the CrN layer did not negatively affect PV module performance.

The conclusion is that the intrinsic silicon, I, layer, the main absorbing layer, too thick to allow significant light to pass through. It is estimated that this layer is as much as 20% too thick. Because the thickness of this layer is a major factor in the current generation and changing it introduces a large number of other variables and interactions, this direction of development will be left to future work.

Aluminum Texture

The angle at which light travels through the photovoltaic material will be relatively orthogonal to the surface of the material with respect to the angle at which it entered. This is non-ideal, because it significantly reduces the path length for the light to reach the bottom of the cell, and return to the surface, figures 3.2.8.

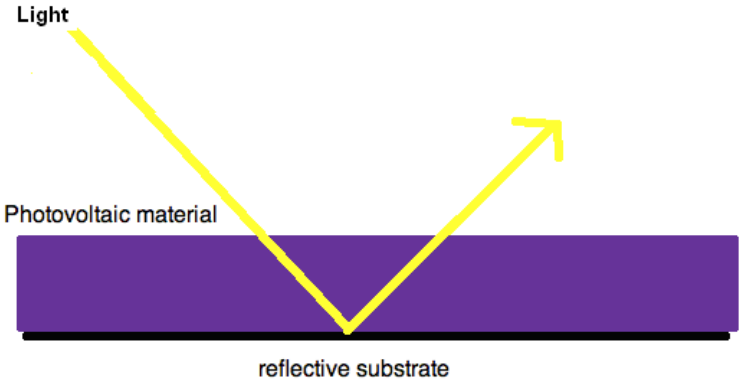

Figure 3.2. 8. Schematic diagram of the light path in a solar module with a perfectly reflective substrate.

The path length of the light can be increased significantly, however, by texturing the substrate, figure 3.2.9. When the light gets reflected by the bottom of the cell it is likely to take an oblique angle and travel through much more PV material. This makes it more likely that each photon will be absorbed. The more photons get absorbed, the more current the module generates. So, a textured substrate will produce more current.

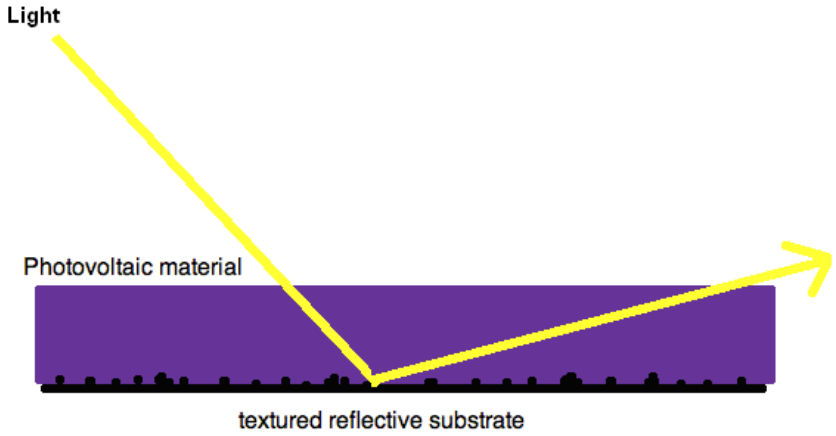

Figure 3.2.9. Schematic diagram of the light path in a solar module with a textured reflective substrate.

Metallized substrates were produced and examined using scanning electron microscopy figures 3.2.10 through 3.3.14. Then the properties of the resulting modules were correlated with the observed microscopic features.

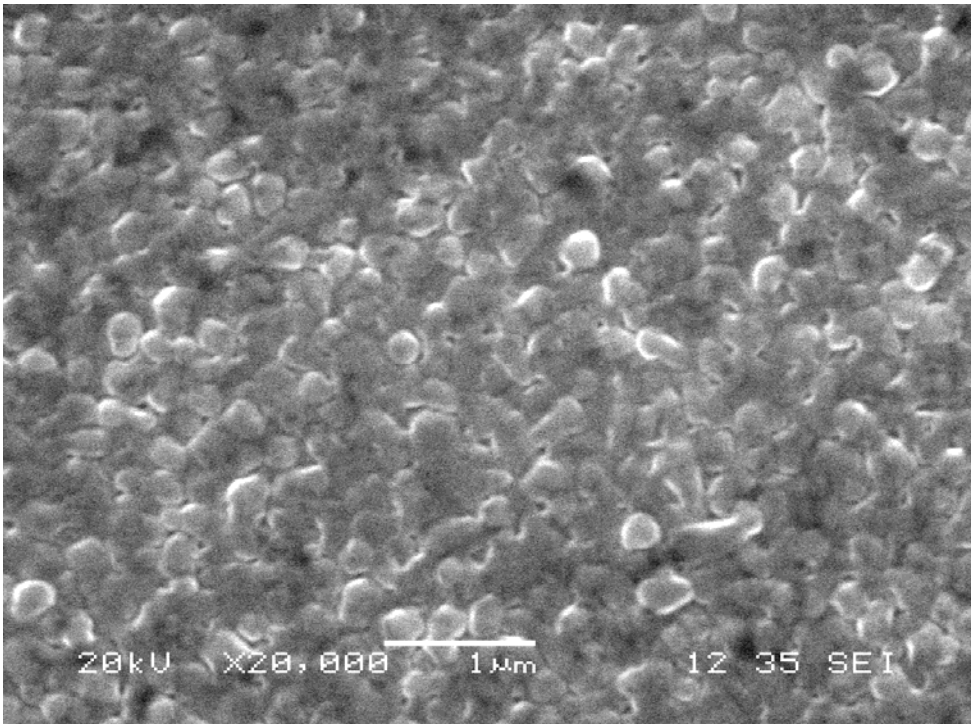

Figure 3.2.10. Substrate texture as deposited using standard conditions.

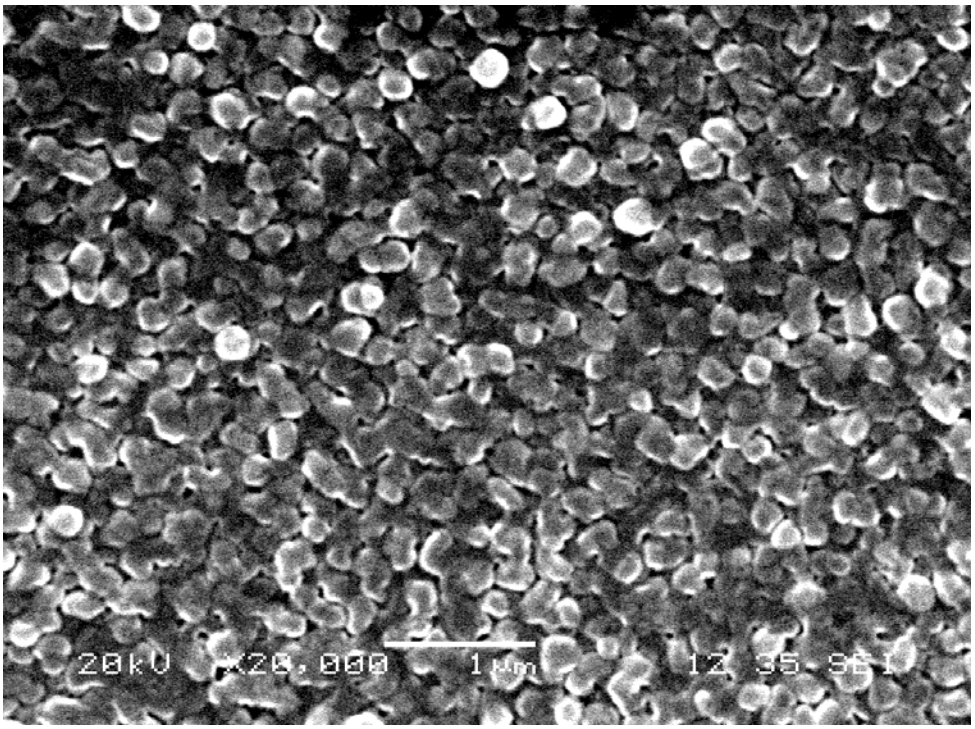

Figure 3.2.11. Substrate texture as deposited at lower temperature.

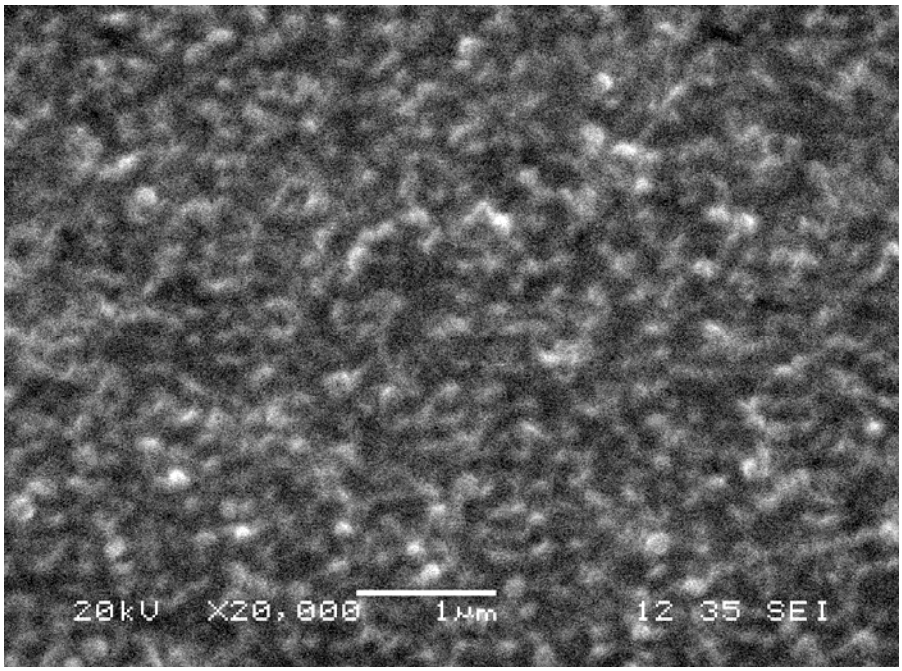

Figure 3.2.12. Substrate texture for material that spent 1/2 of the normal time in the deposition zone.

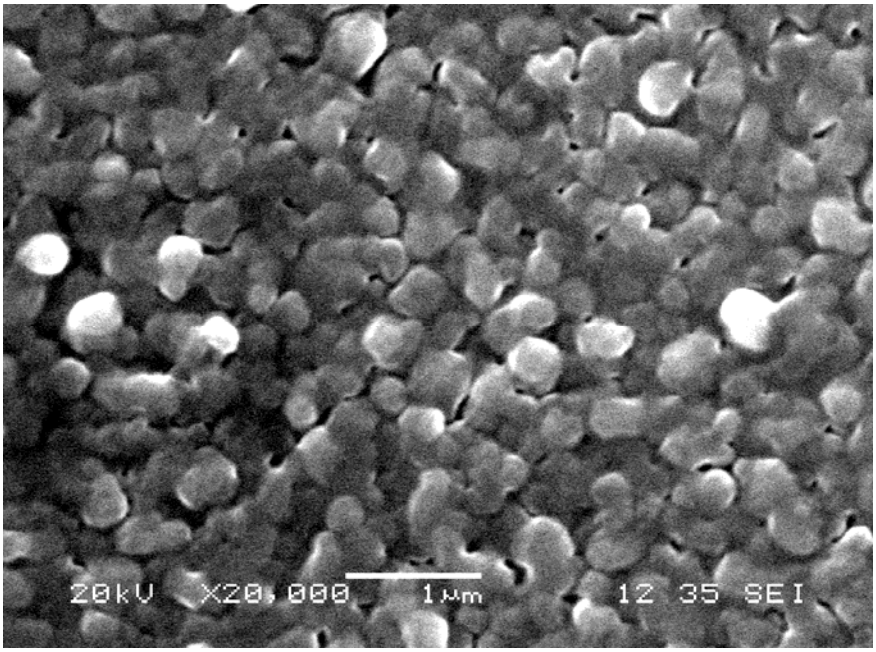

Figure 3.2.13. Substrate texture for material that spent twice as long as normal in the deposition zone.

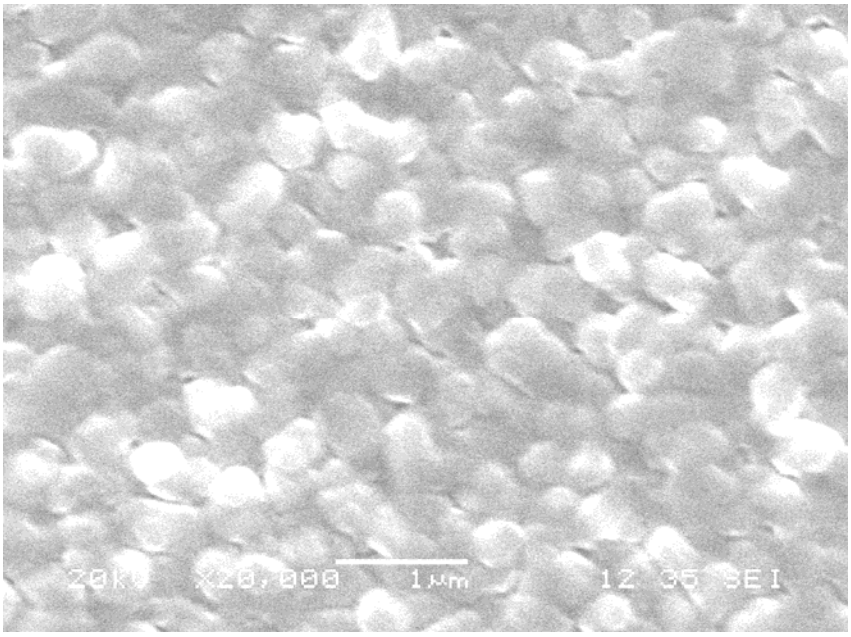

Figure 3.2.14. Substrate texture for material deposited at an elevated temperature.

The scale bars were used to estimate an average feature size, and then these sizes were correlated with the closed circuit current and open circuit voltage of the devices.

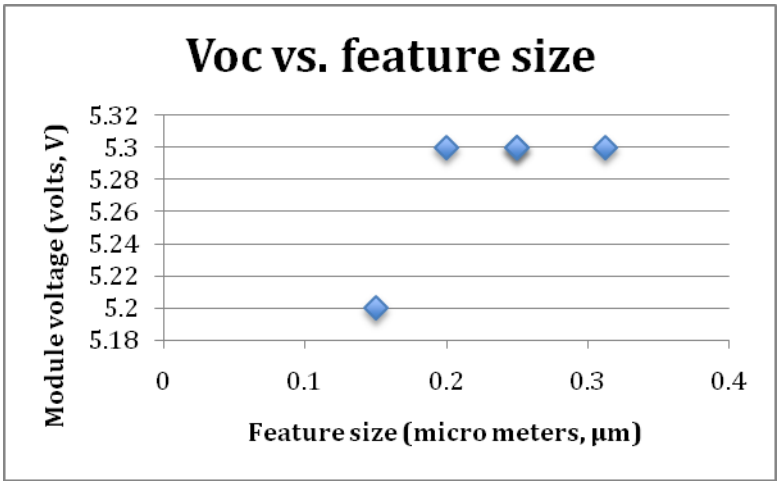

Figure 3.2.15. Open circuit voltage, Voc vs. texture feature size. The low Voc at very low feature size is believed to come from an unrelated phenomenon, and is not considered a part of the trend.

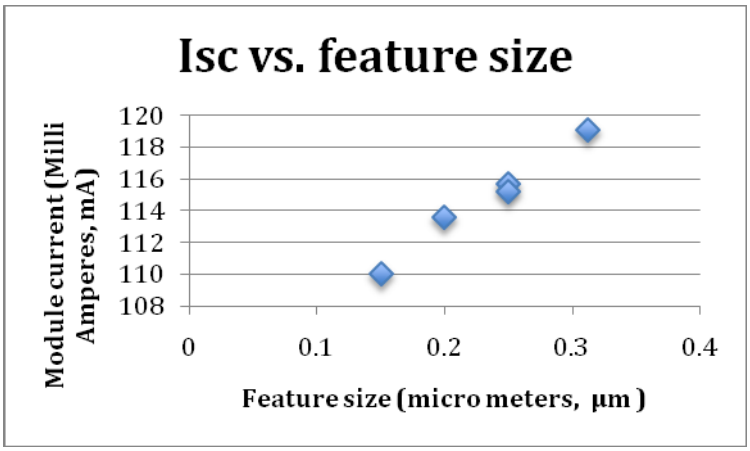

Figure 3.2.16. Short circuit current, Isc vs. texture feature size.

The texture feature size has a significant impact on device current, figure 3.2.16. This is at no apparent loss to the open circuit voltage, figure 3.2.15.

It is clear that the by increasing the texture feature size of the reflective substrate it can have a significant and beneficial impact on device performance in the form of increased current generation at no loss in voltage or change in fill factor.

Unfortunately, the best texture was created by decreasing the speed of the process, which would significantly increase production cost. Initial results show that device performance can be improved by changing the substrate texture, but more work needs to be done in order to make such improvements cost effectively. Additionally, the increased texture was produce by depositing metal films of significantly greater thickness which lead to a high incidence of fracturing of the PV stack. These crack cause device failure with normal process handling leading to high yield losses.

3.3 Incorporate the best solutions into a PV module and run comparative testing against standard modules.

There were no solutions found that could be integrated into our standard PV product.

Task 4: I-Layer/ P: I Interface Improvement

The intrinsic, I, layer of the PV, photovoltaic device, is the current generating layer. When a light photon is absorbed by this layer, charge carriers are generated. Proper thickness and crystal structure are essential for optimum performance of the PV device. The highest efficiency solar cells are dependant on the fabrication of the boundary between this amorphous silicon I-layer and the nano-crystalline P+ silicon layer

4.1 Establish deposition characteristics of the I layer for each electrode in the new, multiple electrode system considering deposition rate and rate at which the deposition moves to the more ordered "proto-crystalline" and micro-crystalline structures. This will be evaluated particularly relative to power and hydrogen dilution.

Within the meter wide machine, the I1 box contains three antennas. It was determined that for proper deposition rates, all three antennas are required. Additionally, cross web uniformity is within 8% until about 3" from the edge. Wider antennas and reconfiguring the RF power lines have brought this uniformity to 5% with in 2" from the edges. Higher silane flow improves the uniformity and it has been found that to maintain sufficient uniformity, the required silane flow produces a higher deposition rate. To maintain proper and uniform film thickness, the required minimum web speed is near 4.5"/min.

Differential flows between antennas indicated no preference for the PV performance. Again the changes affected the generation and path of dust with the best conditions were uniform gas flows to all three antennas.

The I2 box incorporates two antennas. It was found that only one antenna is needed to maintain proper deposition rate. Uniformity is maintained within this box to within 3% across the web. Silane flow affects the uniformity at the edges where as the RF power affects the uniformity in the center areas. The minimum web speed, based on deposition rate as in the I1 box, has been found to be 3.5"/min.

4.2 Determine effects of differential gas flows through the different electrodes and effective mixing of gases in the system for the gas concentrations and silane depletion appropriate for intrinsic a-silicon deposition. This will be used to identify whether a physical barrier is needed between electrodes to achieve differentials in silane partial pressures between areas.

There appears to be no reason to have a physical barrier between the antennas within the I1 deposition zone. There was no indication that control of the process or that the PV material was improved as a result of the isolation bars. Additionally, they tended to cause irregular deposition of dust on the antennas. Although this did not appear to decrease the PV performance, the dust issue caused concern and the bars were removed.

The I2 box performed with a single antenna and so the isolation bar was removed.

4.3 Develop parameters that moves the film structure to the more ordered "proto-crystalline" and micro-crystalline and establish how deposition parameters may be used to control that transition.

Tandem solar cells have two junctions that both add to the overall voltage of the solar cell. Each junction has an amorphous intrinsic or "I-layer" where the positive and negative charges are generated. The thickness and material structure of the I-layers are critical to the performance of the device. Since a tandem cell has two junctions, it also will have two I-layers, which will be called I1 and I2. The thickness of the I1 and I2 layers are critical in a tandem junction solar cell. The two layers should be deposited at thicknesses that allow approximately the same amount of current to be generated in each I-layer. In a tandem cell, the output current is limited by which ever I-layer is generating the least amount of current. The performance is dependant on the material's structure

with the material with the most favorable structure for our solar cells will yield the highest efficiency solar cells.

At Power Film the amorphous silicon PV material is deposited using an RF enhanced CVD process. In these systems the same gases are used to deposit nano-crystalline silicon as amorphous silicon, with the difference being the deposition conditions such as power, pressure, and dilution ratio. Deposition of nano-crystalline silicon typically involves higher dilution ratios and higher powers. Additionally, temperature and pressure are important parameters.

Measurements of the layer thickness, open circuit voltage, Voc, the short circuit current, Isc, the fill factor, FF, the series resistance, Rseries, and the shunt resistance, Rshunt, will be used to assess each parameter.

Power and gas flows were found to have little effect on the performance as measured by fill factor, FF, and open circuit voltage, Voc, for hydrogen dilution between the ranges of from 8 to 12:1 H2:SiH4 dilution, figures 4.3.1.1and 4.3.2. It was learned that the silane flow can improves the uniformity at the outer edges of the deposition zone, although with a decrease the uniformity in the center area. Additionally RF power improves the uniformity in the center but has little effect on the edges. The total combined flow of silane and hydrogen has little effect on uniformity with a small decrease in deposition rate at high total flows. By balancing the RF power with the gas dilution, silane flow, cross web uniformity was improved. For the minimum deposition rate at conditions required to maintain good uniformity, the minimum web speed for the proper deposited film thickness was 3.5”/min. This translates to a 16% improvement in through put over the 13 inch machines.

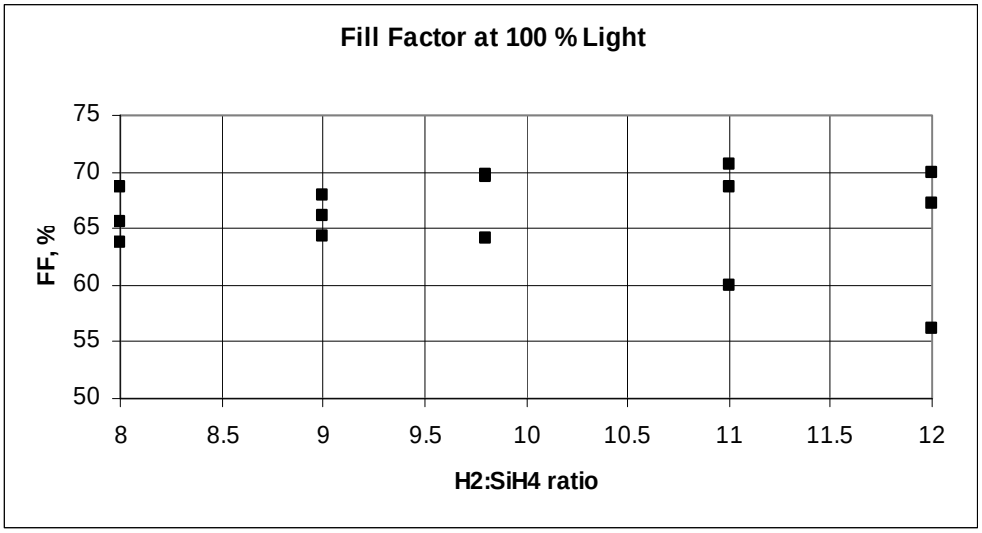

Figure 4.3.1. Fill factor as a function of the hydrogen-silane ratio.

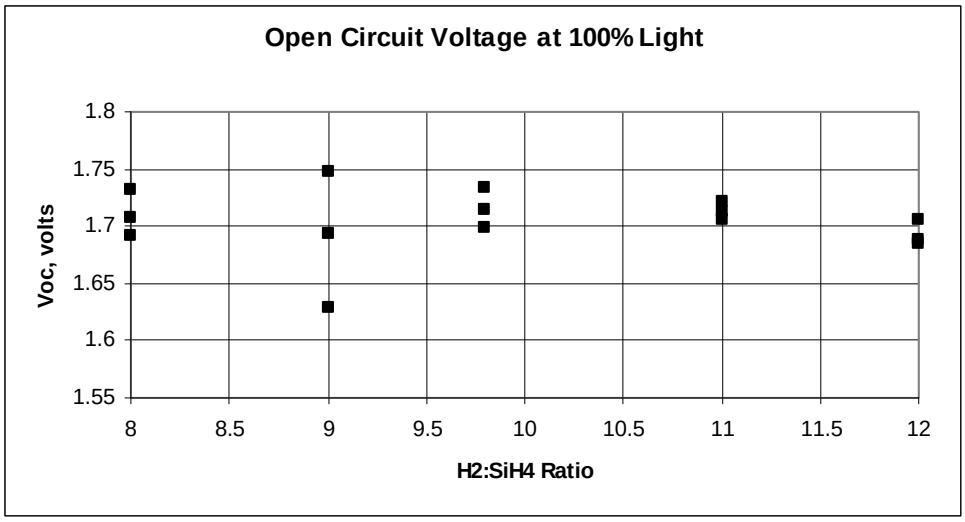

Figure 4.3.2. Open circuit voltage as a function of the hydrogen-silane ratio.

This material was sampled through 3 weeks of light soaking and it was found that the total power output from modules degraded. The best of these samples showed a 33% loss in total power. All frames sampled degraded similarly showing a slight drop in Voc and large drops in Isc and FF, table 4.3.1 through 4.3.4.

Voc, V	Pre-Soak	Post-Soak
Frame 76	20.1	18.8
Frame 84	20.6	19.2
Frame 91	20.6	19.7
Frame 99	20.5	19.2

Table 4.3.1. Light soaking data for Voc.

Isc, mA	Pre-Soak	Post-Soak
Frame 76	82.2	68.7
Frame 84	82.5	70.3
Frame 91	82	69.9
Frame 99	82	69.3

Table 4.3.2. Light soaking data for Isc.

FF	Pre-Soak	Post-Soak
Frame 76	59.2	49.9
Frame 84	64	52.4

Frame 91	64.5	52.4
Frame 99	64.3	53.6

Table 4.3.3. Light soaking data for FF%.

Power, mW	Pre-Soak	Post-Soak
Frame 76	976.97	644.1
Frame 84	1088.5	708
Frame 91	1090.6	723.6
Frame 99	1079.7	714.5

Table 4.3.4. Light soaking data for FF%.

These results indicated significant deviation from optimum performance. Light soaking is primarily affects the intrinsic layers, particularly the I1 layer because of its greater film thickness. Additionally, the level of crystallinity can affect the light stability of the material.

Raman spectroscopy was used to study the nano-crystallinity of the I2 layer. In this layer, the hydrogen to silane dilution ratio was increased from a ratio of 14:1, which is used for Power Film's production cells, up to 50:1. Raman measurement began detecting silicon crystals at a dilution ratio of 32:1. Using this information tandem solar cells were produced and tested with the I2 layer thicknesses varied across this range of dilution ratios. It was found that as the dilution ratio increased the open circuit voltage, Voc, and short circuit current, Isc, of the solar cell quickly decreased, figure 4.1.3. This decreasing relationship suggests that the Raman signal to be scattered away from the detector due to the device structure and is able to detected low nano-crystal fractions. Because of this it was determined that Raman cannot be reliably used on our devices to determine the amorphous-nano-crystalline silicon transition point and that PV module made from lower dilution ratios and then tested for Voc and Isc is the best solution for determining optimal material structure. Samples with dilution ratios from 14:1 to 6:1 show an improvement from 14:1 down to 8:1 with the Voc increasing, but lower then 8:1, the Voc again begins to decrease. This indicates that the optimum dilution ratio for depositing an amorphous silicon I2 layer in Power Film's deposition systems is about 8:1, figure 4.3.3.

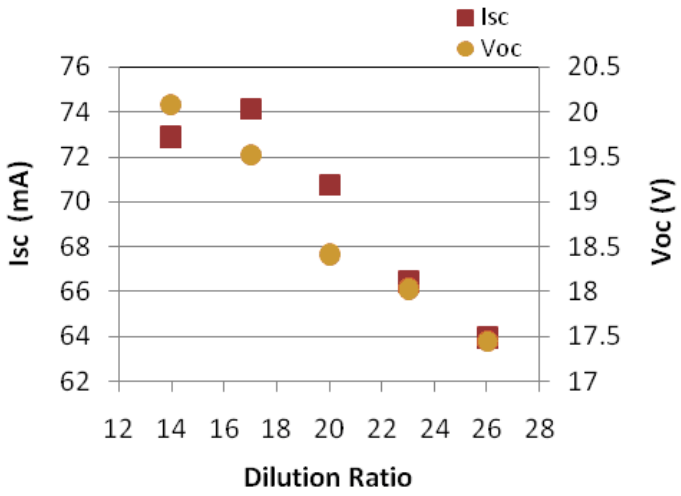

Figure 4.3.3 PV module performance as a function of hydrogen dilution ratio fro the I2 layer.

Using this information, the optimum RF powers and pressures for depositing the I2-layer were determined. The relationship between power, Voc, and Isc can be seen in figure 4.3.4. The optimum conditions for depositing the I2 layer was found to be a dilution ratio of 8:1, power between 165 and 185W, and a pressure between 425 and 525mT.

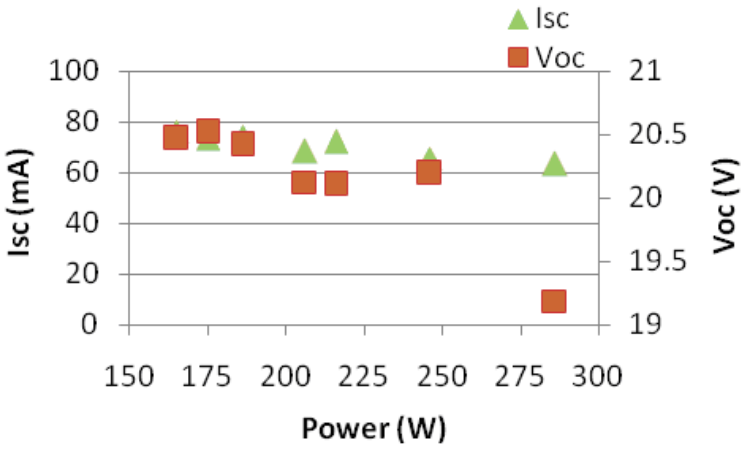

Figure 4.3.4 PV module performance as a function of RF power for the I2 layer.

The I1 layer was investigated in a like manner for the performance dependence of pressure, dilution ratio, and RF power.

The RF power tended to decrease the fill factor indicating that the RF power should be kept low were as the FF was independent of the hydrogen dilution, figures 4.3.5 and 4.3.6.

The open circuit voltage is fairly constant, until a dilution ratio of about 5.5 where causes the open circuit voltage to decrease, figure 4.3.7.

The open circuit voltage increases slightly as the power is increased to 275W until a power beyond 275W is reached where it begins decrease, figure 4.3.8.

The short circuit current increased slightly as the power is increased up to 295W with a loss above that level, figure 4.3.9.

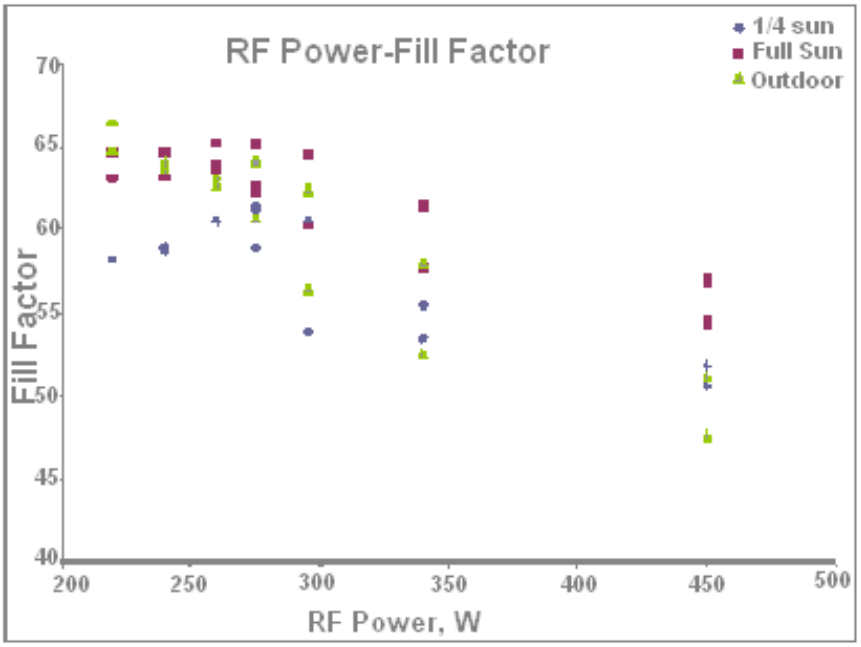

Figure 4.3.5 PV module FF as a function RF power..

.

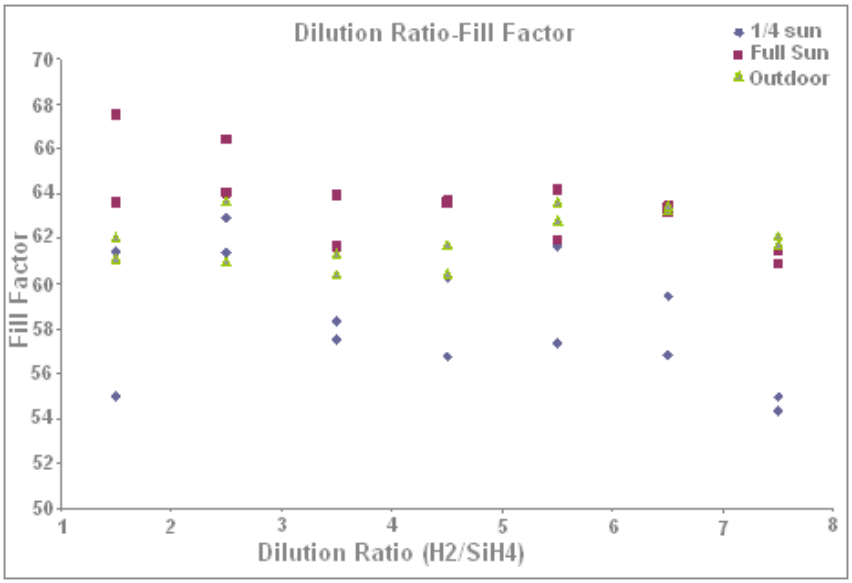

Figure 4.3.6 PV module FF as a function of hydrogen dilution

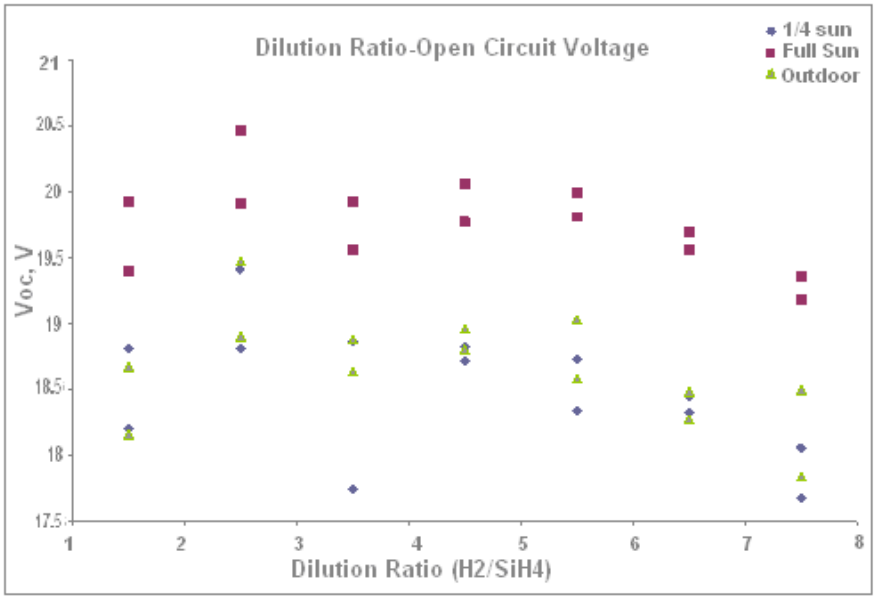

Figure 4.3.7 PV module Voc as a function of hydrogen dilution..

.

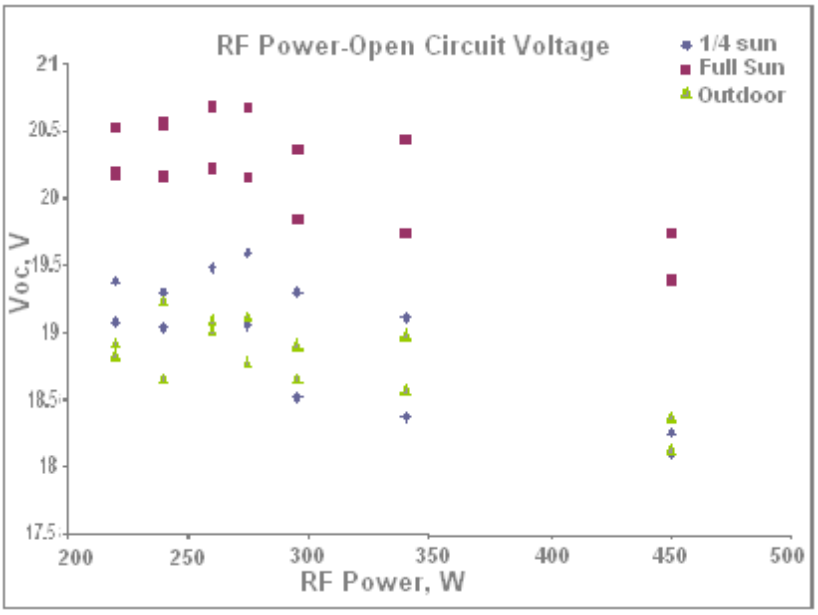

Figure 4.3.8. PV module Voc as a function of RF power

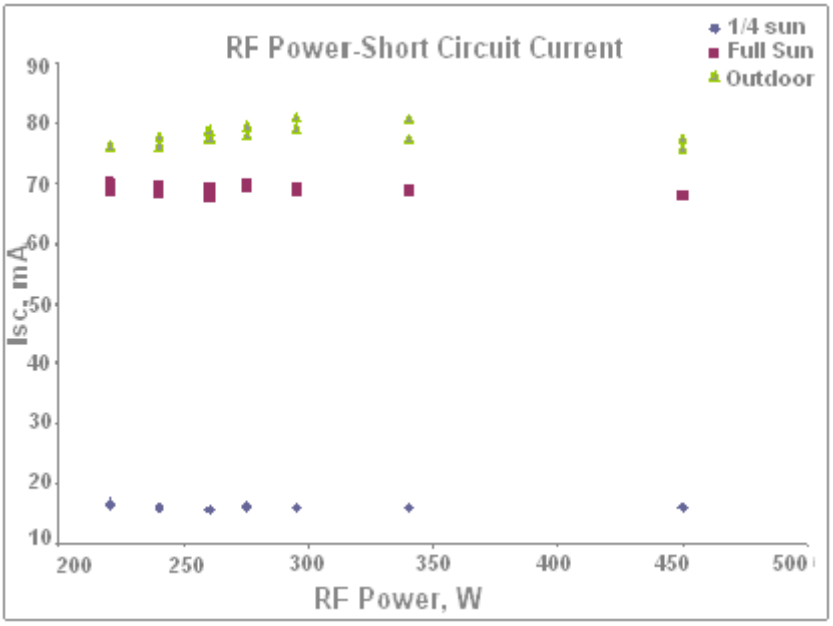

Figure 4.3.9 PV module Isc as a function of RF power

4.4 Apply parameters developed in 4.3 to the final electrode in the multiple electrodes, I layer deposition zone to create a proto-crystalline layer at the top interface of the I-layer. Develop optimum rate parameters to optimize voltage in

full devices. Identify parameter limits needed to protect against overshooting to a microcrystalline structure that would cause voltage to drop dramatically.

From the above information, the optimum RF powers and pressures for depositing the I2-layer were determined. The relationship between power, Voc, and Isc can be seen in figure 4.3.4. The optimum conditions for depositing the I2 layer was found to be a dilution ratio of 8:1, power between 165 and 185W, and a pressure between 425 and 525mT.

Also identified were the conditions for the I1 layer with the optimum being a dilution ratio of 8:1, power between 165 and 185W, and a pressure between 425 and 525mT.

Although these are the optimized conditions, the acceptable range of each is broad enough to be handled by the current equipment which is specified as control with in +/- 5% accuracy.

Task 5. Module fabrication using improvements

Note: There is a possibility that all improvements or improved processes are not inter-compatible and that the final 'best' device module may not contain a totality of these efforts.

The multi antenna design in use in the meter wide machine with the maximize performance of the P+ material was not fully compatible with intrinsic layer development .because the uniformity on this machine is dependant on balancing the RF power with the hydrogen and silane gas flows, limiting the ability to target the dilution ratio and optimum RF power levels.

5.1 Produce and test a PV module with the best solution identified and developed for the top conductive oxide.

Modules were produced, tested and found to pass the damp heat qualifying test.

5.2 Produce and test a PV module with the best solution identified and developed for the P+ layer.

Material with the best P+ material available have been produced.

5.3 Produce and test a PV module with the best solution identified and developed for the red response.

There was no solution found for the best back reflector, with the standard back material remaining unchanged.

Material with the optimum I-layer thickness are found, modules have been produced.

5.4 Produce and test a PV module with the best solution identified and developed for the improved I-P+ interface.

Modules were produced using the multi antenna system in the meter wide machine and demonstrated to pass minimum production tests. Because of the improvement in the rate at which the P+ material can now be deposited, production rate through this machine surpasses the older silicon machines by 50%.

5.5 Compile all of the inter-compatible improvements into a single module.

Material was produced using the 13 inch wide machine so that the nano-crystalline structure developed could be utilized as the PV source material.

Task 6 Fabrication of tent deliverable

The purpose of this task is to produce a useful structure using improved PV device modules.

6.1 Fabricate and a 2KW PowerShade using the PV modules produced in 5.5.

Material was produced in 5.5 was manufactured into a 2KW Power Shade with the delivery point designated by the ARO Contracting Officer's Representation.